Journal of Nuclear Materials 386–388 (2009) 852–855

Contents lists available at ScienceDirect

Journal of Nuclear Materials

journal homepage: www.elsevier.com/locate/jnucmat

3D-AP and positron annihilation study of precipitation behavior in Cu–Cr–Zr alloy

M. Hatakeyama [a,*], T. Toyama [a], J. Yang [b], Y. Nagai [a], M. Hasegawa [a,b], T. Ohkubo [c], M. Eldrup [d], B.N. Singh [d]

[a] The Oarai Center, Institute for Materials Research, Tohoku University, Oarai, Ibaraki 311-1313, Japan
[b] Cyclotron and Radioisotope Center, Tohoku University, Aoba-ku, Sendai 980-8578, Japan
[c] National Institute for Materials Science, 1-2-1 Sengen, Tsukuba 305-0047, Japan
[d] Materials Research Department, Risø National Laboratory, Technical University of Denmark, DK-4000 Roskilde, Denmark

A B S T R A C T

Precipitation behavior in a Cu–0.78%Cr–0.13%Zr alloy during aging and reaging has been studied by laser-assisted local electrode three-dimensional atom probe (Laser-LEAP) and positron annihilation spectroscopy (PAS). After the prime aging at 460 °C, Cr clusters enriched with Zr were observed. Further reaging at 600 °C caused the clusters to grow to almost spherical (1 h) and thick platelets (4 h) Cr precipitates. Zr and impurities of Si and Fe were concentrated around the Cr precipitates, resulting in almost pure Cr cores sandwiched with interface regions enriched with Zr, Si and Fe. Probably the strain induced by the incoherency between BCC Cr precipitates with the matrix FCC Cu is relaxed by the enrichment of Zr, Si and Fe. Positron lifetime and coincidence Doppler broadening experiments suggest that vacancy-like defects form and associate with Cr atoms around the interfaces between the precipitates and the matrix.

1. Introduction

Cu–Cr–Zr is considered as one of the candidate materials for the heat sink of the International Thermonuclear Experimental Reactor (ITER) divertor [1,2]. The main problem to be solved is its thermal stability, since the heat treatment during joining procedures of divertor fabrication may cause solution annealing or reaging of the alloy. Thus, the aging processes of the mechanical and physical properties of the ITER-grade Cu alloy after joining has been studied [3–5].

Thermal aging is used to achieve high strength and simultaneously high electrical conductivity of Cu–Cr–Zr alloys [6]. The role of Zr is to improve mechanical properties at elevated temperature without loss of the good thermal conductivities. However, the effect of Zr on precipitation behavior is not well understood [7].

To clarify the precipitation behavior we have employed laser-assisted local electrode three-dimensional atom probe (Laser-LEAP) by IMAGO Scientific Instruments [8] and positron annihilation spectroscopy (PAS). Using Laser-LEAP we have studied three-dimensional atom map distributions of Cr and Zr alloying solutes and of the Fe and Si impurities. The evolution of the Cr-rich precipitates and their incorporation of the solute Zr and the impurities during the prime aging and following reaging are shown. Positron annihilation experiment demonstrates the formation of vacancy-like defects and their association with Cr during the heat treatments. Preliminary results of Laser-LEAP observation have been reported in the previous paper [9].

2. Experimental

Studied material was supplied by Outokumpu Oyj (Finland) and its chemical composition is Cu–0.78wt%Cr–0.13wt%Zr–0.003wt%Si–0.008wt%Fe [10]. Specimens for Laser-LEAP and PAS experiments were chemically polished and then heat treated in the following way. At first the specimens are solution annealed (SA) at 960 °C for 3 h and then water quenched, followed by prime aging (PA) and reaging (RA1 and RA2). The procedures of the heat treatments are listed in Table 1 [10]. The details of Laser-LEAP method are described in Ref. [9]. Laser-LEAP observation was performed at a pulse repetition rate of 250 kHz, a DC voltage ranging from 4 to 9 keV, laser energy of 0.4 nJ and with specimen temperature of about 50 K.

Positron lifetime measurements were carried out using a conventional fast–fast spectrometer with a time resolution of 190 ps at full width at half maximum (FWHM). About 4×10^6 coincidence events were accumulated for each spectrum. The coincidence Doppler broadening (CDB) spectra of positron annihilation radiation were measured with two Ge detectors in coincidence. The details of these methods are described in Ref. [11]. The CDB ratio curves were obtained by normalizing the CDB momentum distribution of each spectrum to that of the defect-free pure Cu or neutron-irradiated pure Cu (1.5×10^{18} n/cm^2 (>1 MeV), ~50 °C). The shape of the ratio curves in the high-momentum regions, typically $>10 \times 10^{-3}$ m_0c, m_0 is the electron/positron rest mass and c is

* Corresponding author.
E-mail address: hatake@imr.tohoku.ac.jp (M. Hatakeyama).

0022-3115/$ - see front matter © 2008 Elsevier B.V. All rights reserved.
doi:10.1016/j.jnucmat.2008.12.266

Table 1
Heat treatments for Cu–Cr–Zr (Outokumpu) alloys [10].

Heat treatment (HT)	Description of applied HT
Solution annealing (SA)	Heated at 960 °C for 3 h followed by water quench
Prime aging (PA)	Heat treatment SA + aging at 460 °C for 3 h followed by water quench
Reaging 1 (RA1)	Heat treatment PA + aging at 600 °C for 1 h followed by water quench
Reaging 2 (RA2)	Heat treatment PA + aging at 600 °C for 4 h followed by water quench

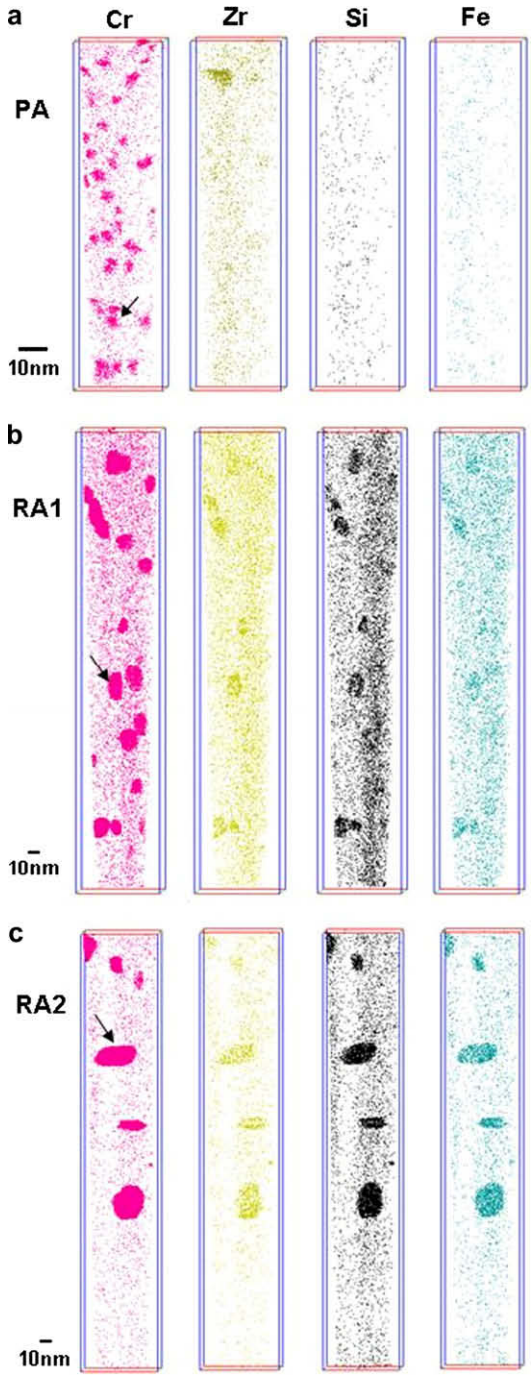

Fig. 1. 2D projection of 3D atom map distributions of the solutes (Cr, Zr) and impurities (Si, Fe) in the Cu–Cr–Zr alloy after (a) prime aging at 460 °C (PA) and reaging at 600 °C for (b) 1 h (RA1) and (c) 4 h (RA2). The atom maps around the precipitates marked by the arrows are enlarged in Fig. 2.

the speed of light) exhibits characteristic signals of the chemical elements through the positron annihilation with their core electrons; these momentum distributions of the core electrons provide the chemical analysis around the positron-trapping defects.

3. Results and discussion

In the SA state of the Cu–Cr–Zr alloy no precipitates were observed by Laser-LEAP. However, after prime aging and reaging, Cr-rich precipitates were observed in the atom map distributions of the solutes (Cr and Zr) and impurities (Si and Fe) in Fig. 1. The number densities and sizes of the precipitates after the heat treatments by our recent Laser-LEAP observation [10] are listed in Table 2. High number density of fine Cr-rich precipitates was observed in the PA state. In the RA1 state the Cr-rich precipitates were coarsened and almost spherical shape with about 10 nm in an average diameter. Zr, Si and Fe impurities were found to have segregated at the Cr-rich precipitates (Fig. 1(b)).

By the RA2 reaging, the Cr-rich precipitates were further coarsened into thick platelets in their shape. Zr and Si impurities were much segregated to the precipitates. The average size of the precipitates increased to about 20 nm.

Fig. 2 shows detailed atom maps around each Cr-rich precipitate in the PA and reaged states marked by the arrows in Fig. 1. In the precipitate of the PA state shown in Fig. 2(a), Zr, Fe and Si impurities are found to be slightly segregated on the surrounding region of the Cr-rich core to form an atmosphere of these impurities In this size of the precipitates the orientation between the BCC Cr precipitates and the FCC matrix is known to be the Nishiyama–Wassermann (N–W) orientation relation in a Cu–0.2Cr alloy [12].

In the RA1 state, the Cr-rich precipitates coarsened as state above and the Zr, Si and Fe impurities furthermore segregated to form enriched layer regions as shown in Fig. 2(b); the spherical Cr-rich precipitates are sandwiched by these two enriched regions. The chemical composition of the enriched regions was estimated to about Cu_7Cr_3ZrSi [9]. Around the center of Cr-rich precipitate the composition of Cr is about 100 at.%. Fujii et al. reported the changing of orientation between Cr precipitate and matrix from (N–W) to Kurdjumov–Sachs (K–S) during the growth of the Cr-rich precipitates on Cu–0.2Cr alloy [12]. Probably the formation of enriched regions seems to be related to this changing of orientation.

In the RA2 state, as stated above, the precipitation has proceeded further; Fig. 2(c) shows a representative atom map around the Cr-rich precipitate with the thick platelet shape. The segregation of Zr and Si around the Cr core of the precipitate is not uniform, which is also due to the misfit between the precipitate and the matrix.

Positron lifetime spectra of the alloy after the heat treatment were well described single lifetime components (Fig. 3); these lifetimes are longer than the positron lifetime of bulk Cu (110 ps [13]) but shorter than that of monovacancies in Cu (173 ps [13]). Thus, they are given by averaged positron lifetimes between the bulk and vacancy-like defects (vacancies and/or dislocations). Usually positron lifetime at dislocations (or dislocation loops) is about 10 ps shorter than that of monovacancies. The lifetimes of about

Table 2
Number densities and sizes of Cr-rich precipitates in the heat treated Cu–Cr–Zr alloys by Laser-LEAP [9].

Heat treatment	Density of precipitates (m^{-3})	Average size of precipitates (nm)
SA	–	–
PA	2.0×10^{23}	2.8
PA + RA1	2.2×10^{22}	9
PA + RA2	5.5×10^{21}	20

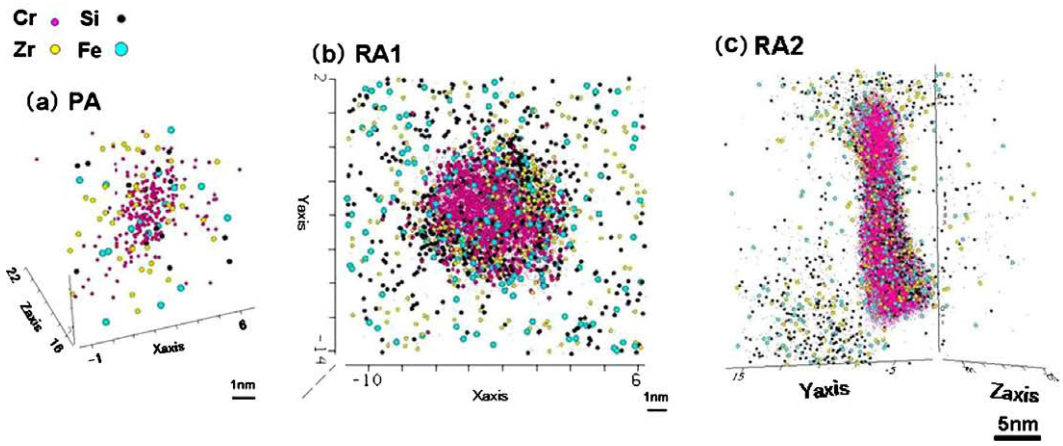

Fig. 2. Atom maps of the solute and impurity distributions in the Cu–Cr–Zr alloy with different heat treatments: (a) PA, (b) RA1 and (c) RA2.

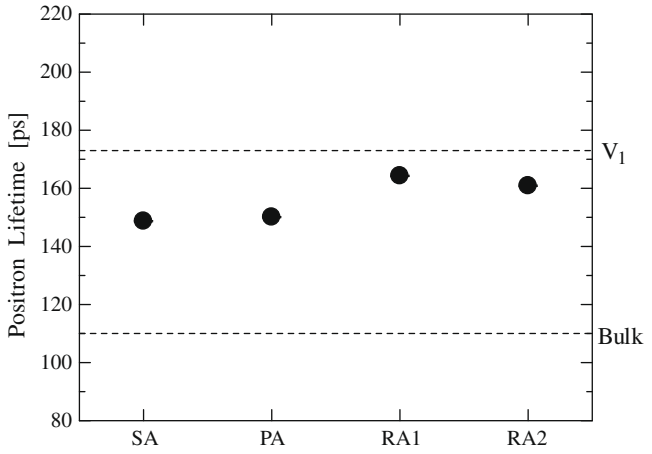

Fig. 3. Positron lifetimes in the Cu–Cr–Zr alloy. The dashed lines show the calculated positron lifetimes for bulk and monovacancies in Cu [13].

150 ps in the SA and PA states suggest that a large fraction of positrons are trapped at monovacancies and/or dislocations induced by these heat treatments. The positron lifetime increased by about 15 ps after the reaging for 1 h (RA1), which is due to monovacancies and/or dislocations induced by reaging?

As shown later, the reaging-induced defects are supposed to be mostly monovacancies formed around the interfaces between the precipitates and the matrix. Then, here firstly we assume that the vacancy-like defects are monovacancies for simplicity. In a two-state positron-trapping model [14], an average positron lifetime τ_{av} between the monovacancies and the bulk is given by:

$$\tau = \tau_B(1 + k\tau_v)/(1 + k\tau_B), \quad (1)$$

where κ is a positron-trapping rate to the monovacancies, and τ_B and τ_V are positron lifetimes in bulk and monovacancies in Cu, respectively The trapping fraction of positrons at the monovacancies is estimated to be about 85% and 80% for the RA1 and RA2 states, respectively, from the trapping rates obtained from Eq. (1). If we assume secondly as the other extreme case that the vacancy-like defects are dislocations, the average lifetimes of about 160 ps suggest that almost all the positrons are trapped at the dislocations. Then, we can say in both the assumptions that more than 80% of the positrons are trapped at the vacancy-like defects induced by the reaging of RA1 and RA2.

Fig. 4(a) shows the ratio curves of CDB spectra, normalized to that of pure Cu, of the heat treated Cu–Cr–Zr alloy together with

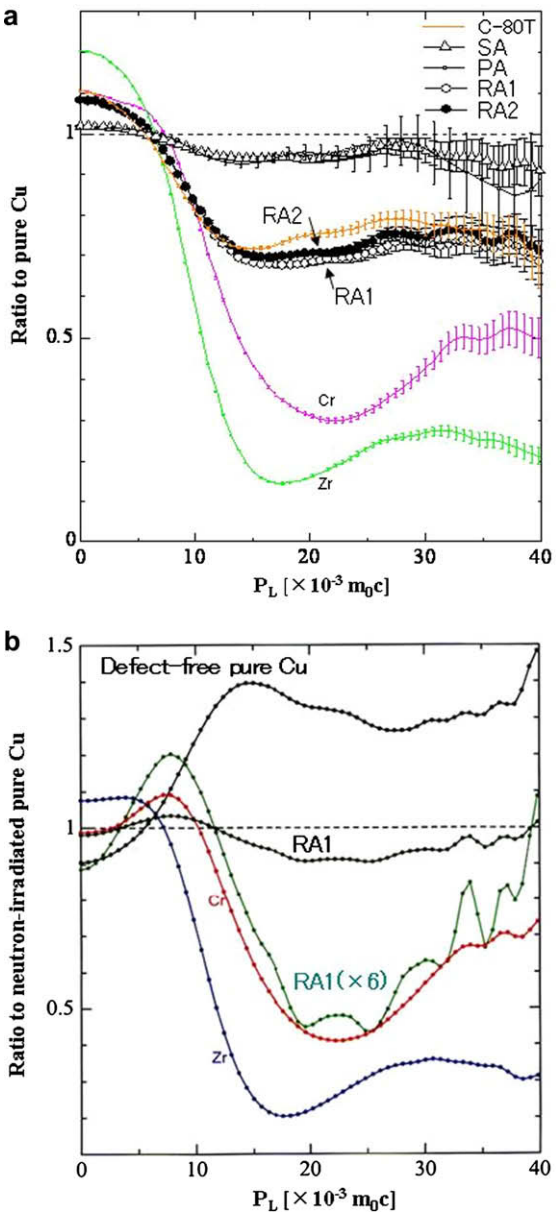

Fig. 4. Ratio curves of the CDB spectra for the Cu–Cr–Zr alloy. CDB spectra are normalized to defect free pure Cu (a) and neutron-irradiated pure Cu (C-80T) (b).

those of pure Cr and Zr as references. Furthermore, that of neutron-irradiated Cu (C-80T) is also shown; its average positron lifetime is about 176 ps which exhibits that almost of all the positrons are trapped at irradiation-induced monovacancies. Small increases at the lower momentum regions accompanied sluggish decreases at higher momentum regions are seen for the curves of the SA and PA states. However, these changes in the ratio curves are markedly enhanced in the curves for the reaged states of Ra1 and RA2, which means the introduction of ample vacancy-like defects by reaging and is consistent with positron lifetime observation stated above.

In the ratio curves of the reaged states, shallow valleys are seen around $20 \times 10^{-3} m_0 c$ in Fig. 4(a). To see the origin of the valley, the CDB spectrum of the RA1 is normalized to neutron-irradiated pure Cu, together with that of pure Cr and Zr as shown in Fig. 4(b). A broad valley centered around $20 \times 10^{-3} m_0 c$ is observed. The ratio curve multiplied by a factor of 6 is found to be very close to that of pure Cr. This shows that about 1/6 (15%) of positrons annihilate with Cr electrons and the remaining 5/6 (85%) of positrons annihilate with Cu electrons. Furthermore, the fraction of positrons which annihilate with Cr electron, I_{Cr}, is estimated for the RA1 and RA2 states, using the fitting of high-momentum part of the CDB ratio curves [15]: 15% for the RA1 and 17% for RA2, respectively.

The above positron lifetime and CDB experiments demonstrate that more than 80% of positrons are trapped at vacancy-like defects induced by reaging and about 15% of them annihilate with surrounding Cr electrons in the reaged states. This suggests that the vacancy-like defects are induced in the interface regions between the Cr-rich precipitates and the Cu matrix in the reaged states.

In Cu–Cr–Zr systems we would expect that the incoherency between the Cr-rich precipitates (BCC) and the matrix (FCC) increase with growth of the Cr-rich precipitates on (K–S) orientation relationship during reaging. If so, Zr and Si and Fe impurities will segregate around the interfaces between the Cr-rich precipitates (BCC) and the matrix (FCC) to form enriched layer regions which relax the strain induced by the misfit between the Cr-rich precipitates and the matrix. Thereby, the relaxation will induce formation of a large amount of vacancy-like defects in the enriched layer regions.

4. Conclusions

The precipitation behavior of the Cr-rich precipitates in a Cu–Cr–Zr alloy during prime aging at 460 °C followed by reaging at 600 °C has been studied by Laser-LEAP and PAS. Our conclusions are as follows:

(1) After the prime aging, high number densities of Cr precipitates are observed and Zr, Fe and Si impurities are slightly segregated to form the atmosphere of them.
(2) By reaging for 1 h (RA1), the Cr-rich precipitates coarsen to almost spherical shape, and the impurities segregate to the Cr-rich precipitates to form enriched layer regions.
(3) Further reaging for 3 h (RA2), the Cr-rich precipitates further coarsen to thick platelet shape and are surrounded the inhomogeneous impurity-enriched regions.
(4) The formation of the enriched layers around the interface regions of the precipitates is ascribed to the incoherency strain between the BCC Cr-rich precipitates and the FCC Cu matrix.
(5) Positron annihilation lifetime and coincidence Doppler broadening (CDB) experiments show that most of positrons are trapped at Cr-associated vacancy-like defects formed around the interfaces between the Cr-rich precipitates and the matrix.

Acknowledgements

This work is party supported by Grant-in-Aid for Scientific Research of the Ministry of Education, Science and Culture (Nos. 17002009 and 15106015). A part of this study was financially supported by the Budget for Nuclear Research of the Ministry of Education, Culture, Sports, Science and Technology, based on the screening and counseling by the Atomic Energy Commission.

References

[1] ITER Joint Central Team, J. Nucl. Mater. 212–215 (1994) 3.
[2] J.W. Davies, D.E. Driemeyer, J.R. Haines, R.T. McGrath, J. Nucl. Mater. 212–215 (1994) 1353.
[3] U. Holzwarth, M. Pisoni, R. Scholz, H. Stamm, A. Volcan, J. Nucl. Mater. 279 (2000) 19.
[4] B.N. Singh, D.J. Edwards, M. Eldrup, P. Toft, J. Nucl. Mater. 249 (1997) 1.
[5] M. Hatakeyama, H. Watanabe, M. Akiba, N. Yoshida, J. Nucl. Mater. 307–311 (2002) 444.
[6] M. Kanno, Z. Metallkd. 79 (1988) 684.
[7] Materials Assessment, ITER Technical Basis, Plant Description Document, p. 8 (Chapter 2.13).
[8] T.F. Kelly, D.J. Larson, Mater. Character. 44 (2000) 59.
[9] M. Hatakeyama, T. Toyama, Y. Nagai, M. Hasegawa, M. Eldrup, B.N. Singh, Mater. Trans. 49 (2008) 518.
[10] B.N. Singh, D.J. Edwards, S. Tähtinen, Risø-R-1436(EN), December 2004.
[11] Y. Nagai, M. Hasegawa, Z. Tang, T. Akahane, K. Yubuta, T. Shimamura Y. Kawazoe, A. Kawai, F. Kano, Phys. Rev. B 61 (2000) 6574.
[12] T. Fujii, H. Nakazawa, M. Kato, U. Dahmen, Acta Mater. 48 (2000) 1033.
[13] H. Ohkubo, Z. Tang, Y. Nagai, M. Hasegawa, T. Tawara, M. Kiritani, Mater. Sci. Eng. A350 (2003) 95.
[14] P. Hautojarvi, C. Corbel, Proceedings of the international school of physics 'Enrico Fermi'. Course CXXV. In: Positron Spectroscopy of Solids, 1995, p. 491.
[15] Y. Nagai, T. Nonaka, M. Hasegawa, Y. Kobayashi, C. Wang, W. Zheng, C. Zhang, Phys. Rev. B 60 (1999) 11863.